

Article

The Effect of Afterbody Geometry on Passenger Vehicles in Platoon

Hesham Ebrahim ^{1,*} and Robert Dominy ² ¹ RWDI, Milton Keynes MK11 3LH, UK² Mechanical and Construction Engineering, Northumbria University, Newcastle Upon Tyne NE1 8ST, UK; Robert.Dominy@northumbria.ac.uk

* Correspondence: Hesham.Ebrahim@rwdi.com

Abstract: It is well known that platoons of closely spaced passenger cars can reduce their aerodynamic drag yielding substantial savings in energy consumption and reduced emissions as a system. Most published research has focused on platoons of identical vehicles which can arguably be justified by some evidence that geometric variety has little to no effect on the overall flow characteristics in platoons of three vehicles or more. It is known that much of the aerodynamic benefit from platooning is gained by the leading two cars, so operating as vehicle pairs could potentially achieve similar environmental benefits whilst addressing many of the practical challenges associated with the safe operation of long platoons on public roads. However, it has been reported that unlike long platoons, the effect of geometry and arrangement is critical if the drag reduction of a pair is to be optimised. This paper describes a parametric study based on three geometric variants of the popular DrivAer model with different combinations and spacings. It is confirmed that vehicle geometry crucially affects the results with the best combinations matching those of long platoons and others creating a net drag increase.

Keywords: DrivAer model; platoon aerodynamics; platoons; bluff body aerodynamics; vehicles in convoy; drag reduction; electric vehicles aerodynamics; aerodynamics



Citation: Ebrahim, H.; Dominy, R. The Effect of Afterbody Geometry on Passenger Vehicles in Platoon. *Energies* **2021**, *14*, 7553. <https://doi.org/10.3390/en14227553>

Academic Editor: Joseph Katz

Received: 25 September 2021
Accepted: 10 November 2021
Published: 12 November 2021

Publisher's Note: MDPI stays neutral with regard to jurisdictional claims in published maps and institutional affiliations.



Copyright: © 2021 by the authors. Licensee MDPI, Basel, Switzerland. This article is an open access article distributed under the terms and conditions of the Creative Commons Attribution (CC BY) license (<https://creativecommons.org/licenses/by/4.0/>).

1. Introduction

The concept of passenger cars operating in low drag platoons is well established (e.g., [1,2]), but it has been recent developments in inter-vehicle communication and smart/autonomous vehicle (AV) capability that have brought the concept closer to reality. Almost all major manufacturers expect to bring such vehicles to the market within the next few years [3,4] and the development of platooning has gained impetus by its potential to increase the range of electric vehicles that will eventually dominate the market [5].

The automotive industry today is dominated by 14 car companies that control a combined total of 62 brands, each of which has a portfolio of vehicle designs with varying dimensions and geometries [6]. This pool of continuously evolving vehicle designs introduces a large matrix of possibilities in terms of vehicle aerodynamic interactions when operated in a platoon. Much of the existing literature on platooning relates to groups of identical vehicles (e.g., [7,8]) which can be useful to address specific flow or performance details, but real-world platoons are likely to be created from different vehicle types assembled in random order. It has already been established that the potential aerodynamic gains are sensitive to vehicle geometry, the number of vehicles in the platoon, and the spacing between them, but our understanding of the detailed interactions remains inconclusive. Researchers frequently draw conflicting conclusions which are seemingly dependent upon the platoon structure that was selected for investigation and there is evidence that there are some parametric combinations that may even increase the overall drag of the platoon [9].

For an individual vehicle within a platoon, its drag is influenced by its geometry and the geometries of those around it leading to optimisation studies for the ordering of

vehicles in the platoon. The addition of active aerodynamic devices and body morphing to further enhance the drag reduction has also been investigated [10], but despite our rapidly developing understanding of the flow structures associated with vehicles in very close proximity, it is perhaps surprising to note that published data on long platoons of different vehicle types suggest that the overall energy saving of the platoon is not greatly affected by the ordering of vehicles [11].

Despite advances in smart technologies, there remain substantial hurdles to be overcome before platooning can develop from a concept to a practical feature of future road transport. Some issues for which solutions are non-trivial include, but are not limited to, joining and leaving a platoon, sharing the highway with other vehicles, compatibility of communication between vehicles within and outside the platoon, responding to unmapped routes with no road markings, and adaptation for limited visibility weather conditions. In time these issues can and will be solved, but they raise the question of whether most of the gains from platooning can be achieved more simply by adopting very short platoons for which just a pair of vehicles is the limiting case. If they can, then the technology is already largely in place for adoption. Experience from motorsport and particularly the National Association for Stock Car Auto Racing (NASCAR) has shown that pairing (the 2-car draft) is hugely beneficial for both the leading and trailing cars [12] and the implication is that the aerodynamic benefit to the pair is comparable to that of the much longer competing platoon of remaining cars. NASCAR regulations result in a field of almost identical vehicles having a very specific geometry that leads to close racing, so an important question is whether similar benefits can be achieved for passenger cars of different geometry where the aerodynamic design of each vehicle type has been optimised in isolation.

For two-vehicle pairs, it has been reported that the effects of geometry and order have a significant effect on their individual and combined aerodynamic drag, so optimisation is essential [10]. Designs for further improving the efficiency of a vehicle pair have been proposed. For example, a study of NASCAR has shown that introducing passively blown ducts located underneath the headlights would reduce the adverse drag increase on the trailing vehicle at close spacing. These ducts would channel the impinging flow separating off the leading vehicle to the side of the front wheels acting as a wheel curtain, thereby improving the vehicle performance in the platoon without compromising its baseline performance [13]. Other studies focused on the frontal edge radius and concluded that adjusting this parameter could play a significant role in reducing the drag of both vehicles; however, it should be noted that the observed gains were sensitive to the scale of the vehicles tested [14–16].

This paper presents new knowledge and understanding of the aerodynamic behaviour of vehicle pairs based on a parametric study of three afterbody geometries of the popular DrivAer model in which the chosen pair, their order, and their inter-vehicle spacing were evaluated.

2. Methodology

2.1. DrivAer Model

The investigation focused on the DrivAer model published by the Institute of Aerodynamics and Fluid Mechanics at Technische Universität München (TUM) [17] that is based on merging the characteristic curves of two medium-sized cars, the Audi A4 and the BMW 3 Series. This vehicle geometry is ideal for platoon base sensitivity studies as it offers three base configurations, the estateback (EB), fastback (FB), and notchback (NB) which are representative of current production cars. For illustrative purposes, the estateback configuration is shown in Figure 1 with the dimensions presented in full scale as simulated.

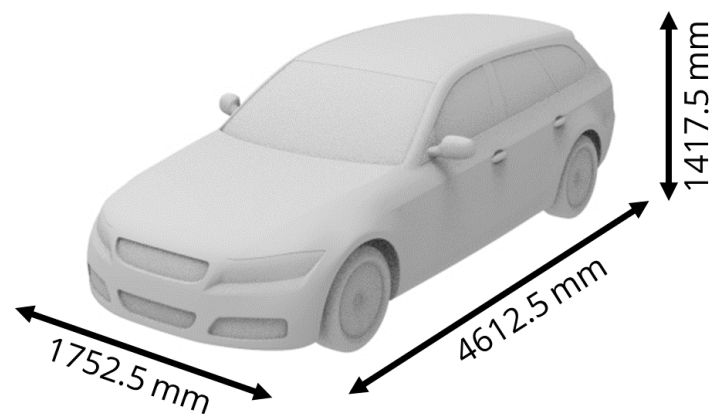


Figure 1. DrivAer model in full-scale.

The level of detail of the grill, radiator, engine bay, wheel rims, and underbody was kept to a minimum to focus primarily on the base changes that would have the most influence on platooning. Each of the three base configurations was simulated in pairs, in a different order, and at different inter-vehicle spacing. The spacing was varied in increments of 25% of the vehicle length (i.e., 0.25 L) up to one vehicle length (i.e., 1 L). This resulted in a total of 36 test scenarios to characterise the effect of each base geometry on the overall drag of the platoon and individual geometries within the platoon.

2.2. Simulations

Computational Fluid Dynamics (CFD) simulations were performed using Star-CCM+ (Siemens PLM Software, Plano, TX, USA) with a modelling setup that has been previously validated against on-track [5] and wind tunnel [7] investigations; therefore, the mesh dependency and other boundary conditions are outlined in more detail in those publications. The domain size was sufficiently large to ensure a blockage ratio below 5% and was discretised using a hexahedral grid topology with 15 prism layers adjacent to the DrivAer model surface achieving a $y^+ \leq 1$. The Reynolds number and the distances between vehicles were chosen based on typical motorway driving speeds and potential driving scenarios, respectively. These parameters were developed based on sensitivity studies of vehicles in a platoon to produce an acceptable correlation with experimental measurements. Boundary conditions, solver settings, ground simulation, and turbulence models were consistent with published studies and are summarised in Table 1. Note, the domain size was scaled relative to the base of the trailing vehicle, adjusting the L_R dimension, and that the ground simulation was kept stationary to be consistent with the large body of publications on the DrivAer model in isolation.

Table 1. Simulation settings for the individual and platoon configurations.

Modelling Parameters	Adopted Settings
Reynolds Number	9.66×10^9
Inlet Velocity	30 ms^{-1}
Grid Topology	Hexahedral mesh
Number of Cells	15 M to 40 M
Domain Size ($L_F/L_R/W/H$)	3 L/4 L/3 L/3 L
Near Wall Treatment	Hybrid all y^+ mesh
Prism Layer Count	15 Layers
First Cell Height	3×10^{-5}
Time	Steady-State
Ground Simulation	Stationary
Pressure/Velocity Coupling	Segregated Flow
Equation of State	Constant Density
Viscous Regime	Turbulent
RANS Model	k- ϵ Realizable

For this study, only the drag coefficient was considered according to Equation (1) and normalised against the baseline isolated vehicle drag coefficient (which is referred to as the drag ratio throughout the manuscript):

$$C_D = \frac{D}{0.5\rho_\infty V_\infty^2 A} \quad (1)$$

where, D is the force acting on the body parallel to the flow direction, ρ_∞ is the free-stream density, V_∞ is the free-stream flow velocity, and A is the frontal area of the DrivAer model which remains constant for all three variants.

3. Results and Discussion

3.1. Validation

Additional validation was conducted to confirm that the methodology implemented provides reasonable correlation to published experimental data on the DrivAer model, however, direct comparison between the CFD and experimental data sets was not perfect due to the differences in setups which includes the blockage ratio, boundary layer thickness, model details, and the Reynolds number. When these simulations were performed, they were not intended to assess the validity of different computational models, but rather to understand the trends and effects of different base geometries on a platoon under typical motorway driving conditions.

Figure 2 shows the centreline pressure coefficient C_p of the upper surface for all three base configurations of the vehicles in isolation. For clarity, only the EB geometry has been superimposed to allow the pressure changes to be related to the major geometric features. The simulated centreline pressure results closely match the experimental measurements obtained from [17] up to $x/L = -0.67$ before deviating as the flow approaches the roof where the pressure reaches a minimum. For all three configurations, the pressure up to this point would remain consistent as the front half of the geometry is identical and follows the chorological data of many passenger vehicles of similar dimensions. As the flow travels past $x/L = -0.5$, the pressure curves of each geometry begin to diverge, indicating a pressure recovery behaviour unique to each base geometry. The EB exhibited a rapid pressure recovery compared to the FB and NB over the roof; however, the pressure would remain lower than the FB and NB past the slanted rear window where a steeper pressure recovery was observed. Both the FB and NB geometries have a higher base pressure than the EB, which conforms with the accepted understanding of these geometries. The magnitude of these pressure curves potentially deviated from the experimental measurements due to the mismatch in the Reynolds number, but the specific trend of each base configuration was well captured.

To ensure that the wake structures of each base geometry were also simulated correctly, a comparison was made against the experimental measurements published by [18]. Figure 3 compares the normalised velocity magnitude and in-plane velocity streamlines in the wake at the vehicle centreline. Deviations in the velocity magnitudes are visible between the two investigation methods, which are largely attributed to the differences in geometry details including the engine bay, rims, and underbody roughness as well as the Reynolds number. Despite these differences in magnitudes, the main characteristics of the wake structures of each configuration are well captured.

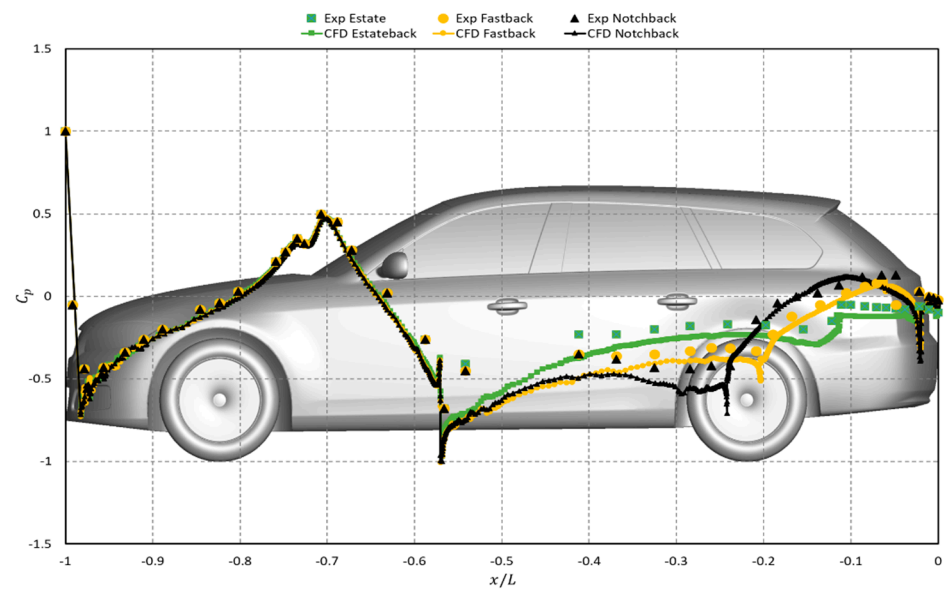


Figure 2. Centreline pressure coefficient comparison between CFD and experimental data obtained from [17] for the EB, FB, and NB geometries.

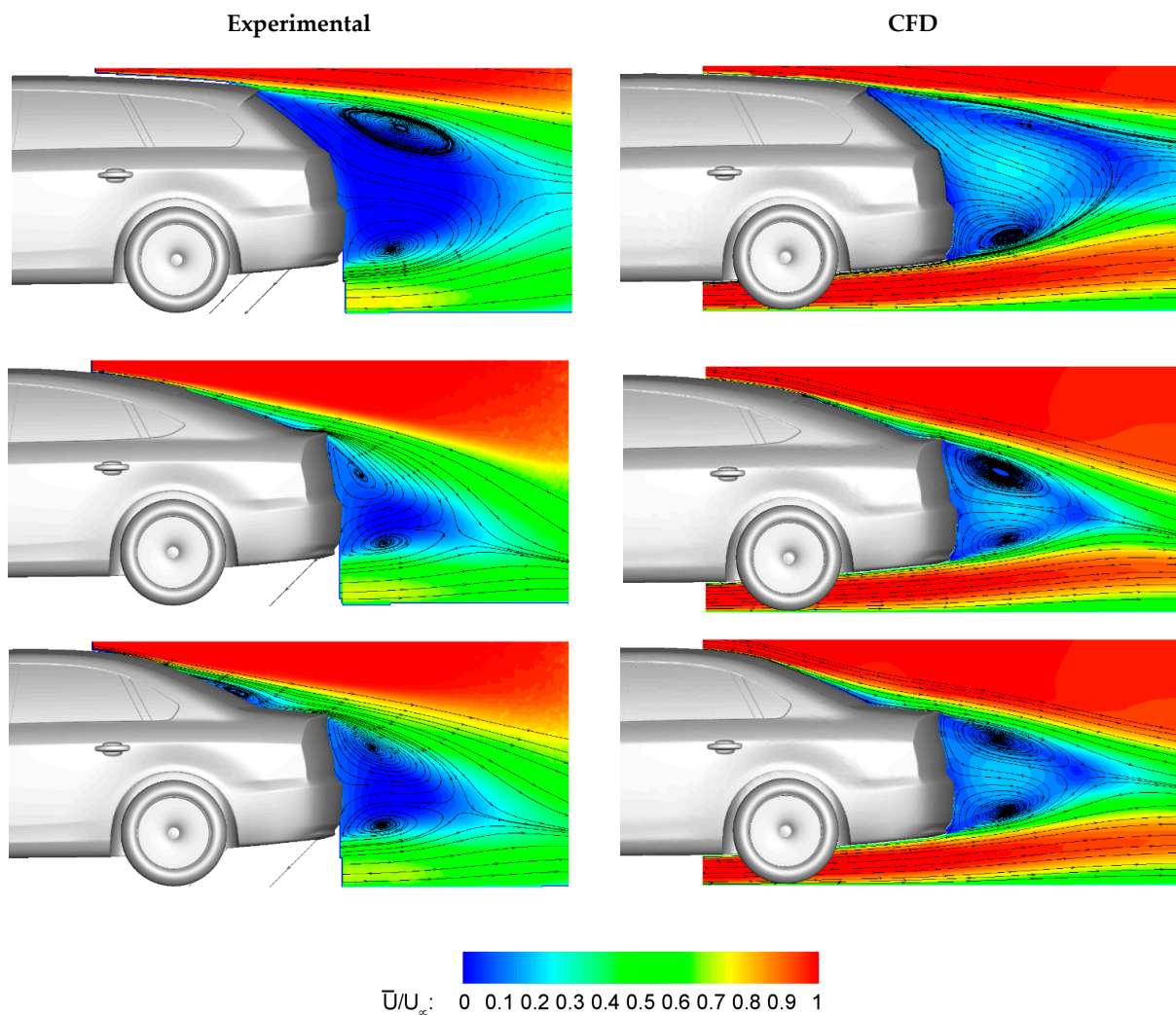


Figure 3. Centreline velocity magnitude plots normalised to free-stream velocity with streamlines in the direction of flow for CFD and experimental results obtained from [18] for the EB, FB, and NB geometries.

The EB forms a large wake as the flow separates immediately at the edge of the rear roof spoiler and underbody diffuser, generating a pair of counter-rotating vortices analogous to squareback geometries. The closure of the wake in the horizontal plane is slightly different from that reported by the experimental measurements due primarily to the underbody flow velocity which drives the flow more aggressively upwards with a tighter free-shear layer separation. The FB and NB geometries produce very similar wake structures at the vertical base that are much shorter in the horizontal and vertical directions compared to the EB. Any variation in the wake is better represented by the three-dimensional view (in Figure 4) which confirms the recirculation bubble present in the NB on the lower side of the slanted rear window that was observed experimentally.

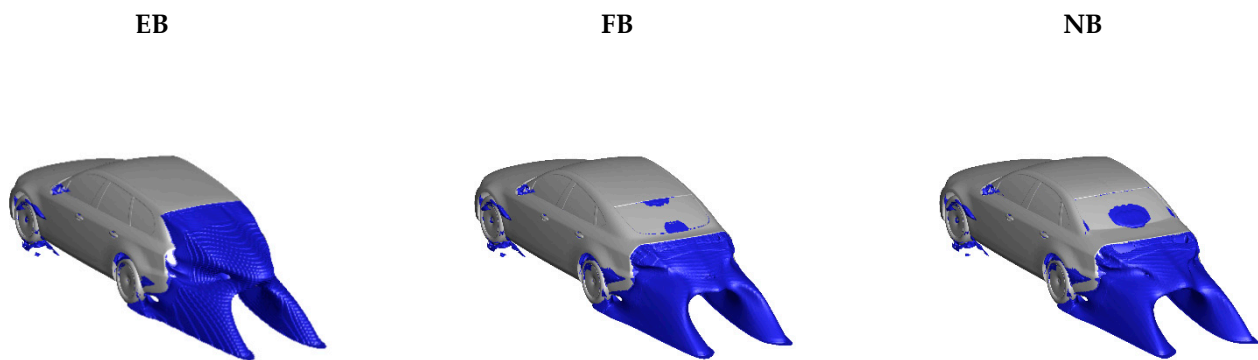


Figure 4. CFD results of the three-dimensional wake structure of the three baseline configurations represented with iso-surfaces of the velocity magnitude below 5 ms^{-1} .

The predicted three-dimensional wake structure of each base geometry is presented in Figure 4, by plotting a flow velocity below 5 ms^{-1} with an iso-surface. This approach shows the wake structure extent of each base geometry and the main features that influence the following vehicles. For the EB geometry, the expected wake is much larger as the flow immediately separates at the sharp edge of the spoiler compared to the FB and NB geometries, where the flow remains attached up to the vertical surface of the base [19]. The wake structures of the FB and NB geometries are comparatively similar, and the only distinct difference was observed on the slanted rear window, where a larger flow recirculation bubble occurs on the NB compared to two smaller zones on the FB geometry. The effect of these changes can be quantified by the C_p curves in Figure 2, which indicate that the base geometry influence extends far forward up to $x/L = -0.4$ and that the centreline pressure of the NB geometry recovers earlier than the FB with a higher magnitude. This ultimately makes the NB geometry the most aerodynamically efficient option compared to the other two geometries as reflected by the drag coefficient results in Table 2. Note that the quoted experimental drag coefficients were averaged based on several publications with similar setups [17–25].

Table 2. Comparison between CFD and experimental drag coefficient results of the three baseline configurations in isolation.

		EB	FB	NB
C_D	Experimental	0.293 (± 0.06)	0.253 (± 0.06)	0.251 (± 0.06)
	CFD	0.291	0.251	0.249

3.2. Two-Vehicle Platoon

The presented results are divided into three sections, each based on one of the three geometries as either the leading or trailing vehicle. In each section, the geometry of the paired vehicle and the inter-vehicle spacing is varied.

The commonality of the results presented for each section in Figures 5–7 is that the leading vehicle drag ratio remains consistent irrespective of the following vehicle base geometry for each inter-vehicle spacing. This is an intentional limitation of these investigations as the frontal half of the DrivAer model is identical, however, for different configurations, the drag ratio would change predictably according to the leading vehicle base geometry.

Velocity and pressure contours were not provided in this manuscript as the observations made were largely similar to those reported in [5,7], which explains the fundamental reasons a trailing vehicle exhibits a drag increase in certain arrangements and spacing. In addition, due to the bespoke nature of this investigation, no experimental research data was found to compare this dataset.

3.2.1. Estateback Geometry

The drag ratios for an EB leading the platoon as shown in Figure 5 (left), would always be favourable and would be expected to increase linearly with the inter-vehicle spacing based on the results from other studies [25–28]. When the order is reversed, i.e., where the EB is following different base geometries as shown in Figure 5 (right), it does not necessarily achieve any energy savings when it is following a FB and/or NB at inter-vehicle spacing of 0.5 L and 0.25 L. This unfavourable effect would dissipate as the inter-vehicle spacing becomes greater than 0.75 L when the leading vehicle wake interaction with the EB is reduced. The effects of the FB and NB on the following EB drag ratios are relatively similar, which is expected given the similarities observed in the wake (in Figure 4). However, with a leading EB, a reduction was observed in the drag ratios on the following EB, despite a noticeable peak at an inter-vehicle spacing of 0.5 L. These observations corroborate with published data on similar EB geometries [7] where this peak was attributed to the increase of pressure drag on the frontal half of the following vehicle due to the leading vehicle flow trajectory that impinges on the following vehicle’s bumper.

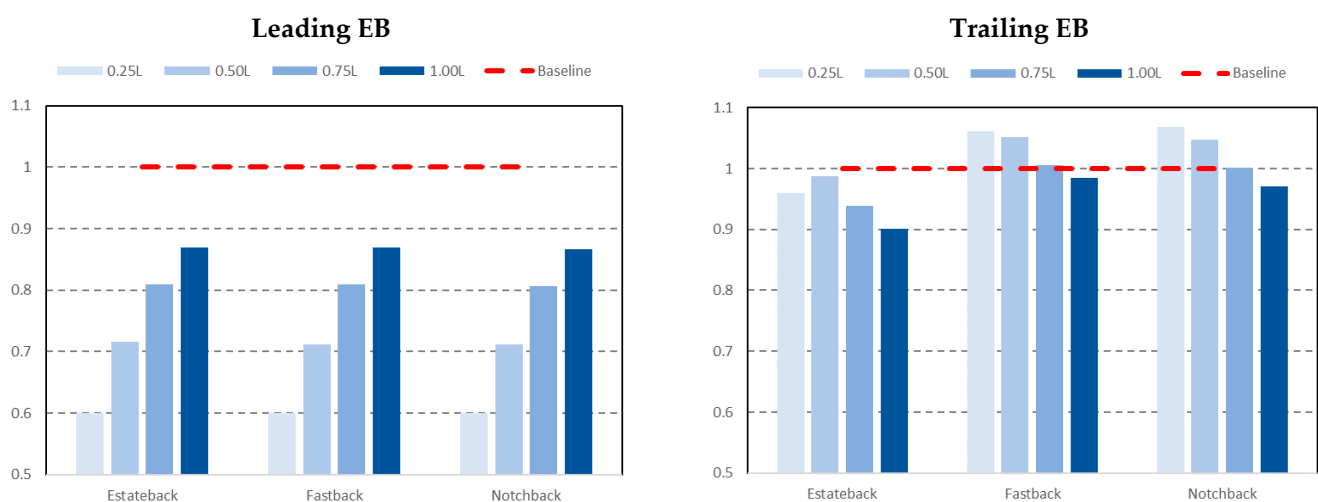


Figure 5. Drag ratios results of a leading EB (left) and a trailing EB (right) in different inter-vehicle spacing and configuration order normalised against the baseline results of an EB.

3.2.2. Fastback Geometry

Similarly, the drag ratios for a FB leading the platoon as shown in Figure 6 (left) would always achieve favourable energy savings regardless of the inter-vehicle spacing tested, but the drag reduction was lower than that reported on a leading EB by approximately 10% across the tested inter-vehicle spacings. This drop in magnitude is inevitable as the baseline drag coefficient of the FB was approximately 14% lower than the EB, and thus any additional drag savings would amount to much higher savings in total. In contrast, the FB

would suffer in the trailing position of a platoon as observed in Figure 6 (right), where the drag ratios would exceed the baseline value in all the tested scenarios.

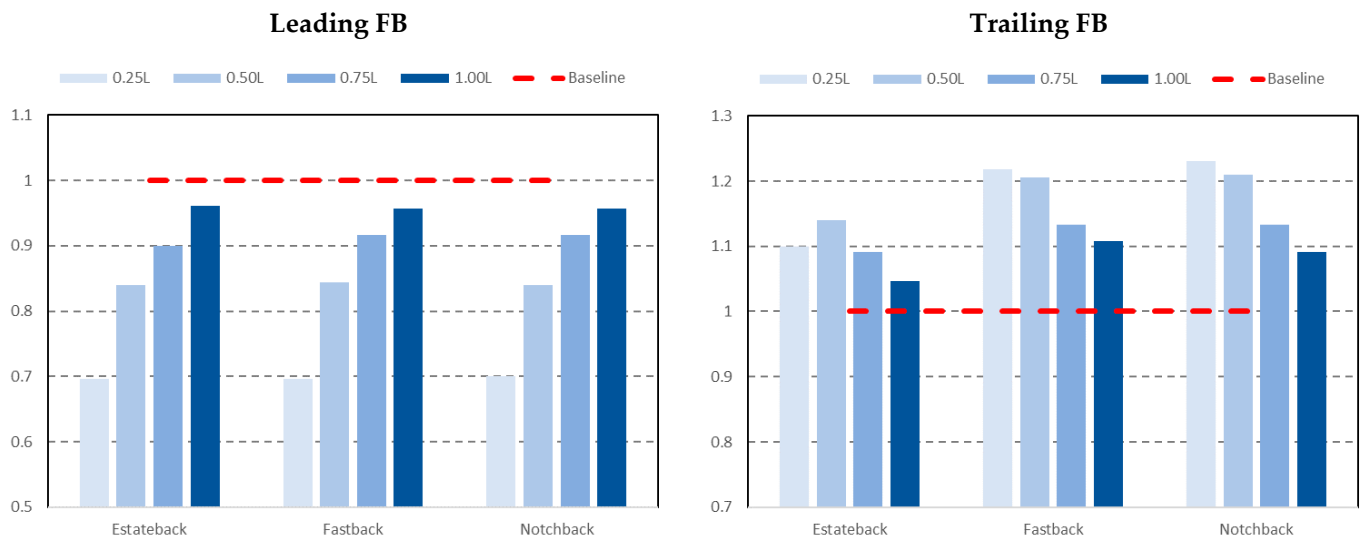


Figure 6. Drag ratios results of a leading FB (left) and a trailing FB (right) in different inter-vehicle spacing and configuration order normalised against the baseline results of an FB.

3.2.3. Notchback Geometry

Figure 7 shows that the results and trends obtained for the NB geometry are unmistakably similar to those observed from the FB geometry with marginal differences in the absolute ratios. This is again expected from the baseline analysis conducted on both geometries which indicated very small differences in aerodynamic performance. Therefore, any conclusions made on the NB geometry are congruous to those made on the FB.

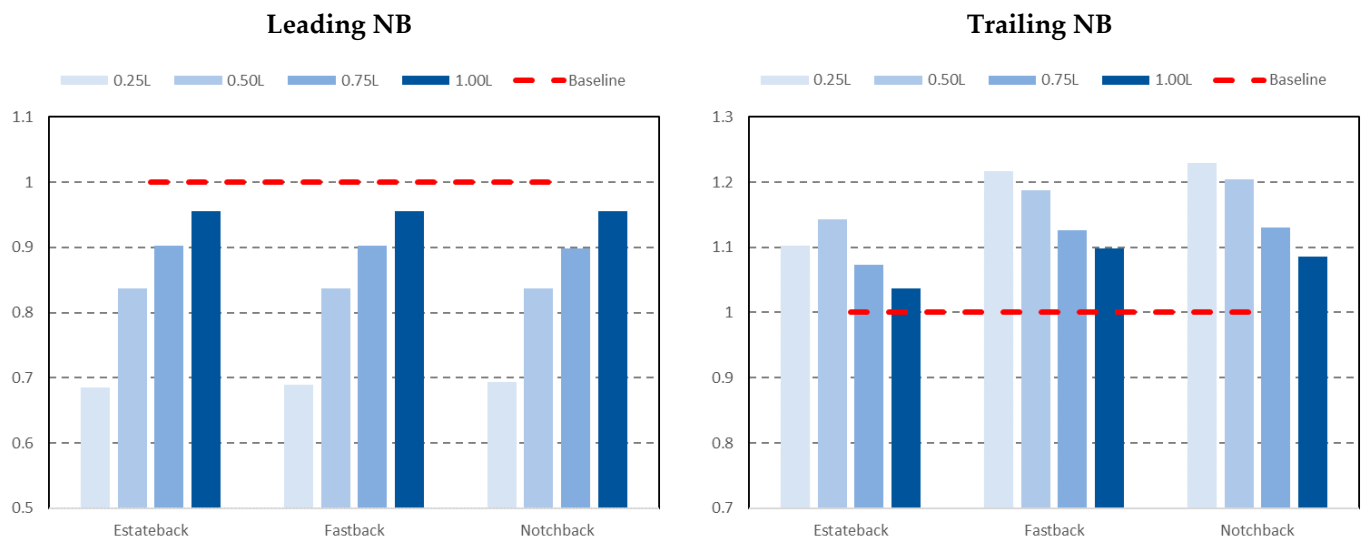


Figure 7. Drag ratios results of a leading NB (left) and a trailing NB (right) in different inter-vehicle spacing and configuration order normalised against the baseline results of an NB.

3.3. Overall Analysis

So far, the analyses were conducted on the performance of individual vehicles within the platoon, but to fully understand the performance of the system, these drag ratios must be coupled. Table 3 summarises and ranks the paired configurations from best to worst

based on the order of geometry, the drag ratio of the system, and the inter-vehicle spacing. The following observations can be drawn from this table:

1. That all the combinations that included an EB geometry would provide favourable energy savings as a system regardless of inter-vehicle spacing and vehicle order;
2. For the FB and NB geometries, energy savings would only occur between these two geometries (irrespective of order) when the inter-vehicle spacing is 0.25 L or potentially lower; and
3. That the best overall drag ratio achieved from these configurations of the DrivAer body is 0.780 where both vehicles have the EB geometry.

Table 3. Summary of the platoon drag ratios normalised against the baseline results of each vehicle ranked to represent the most favourable combinations. C_{DL} is the drag coefficient of the leading vehicle in platoon, C_{DT} is the drag coefficient of the trailing vehicle in platoon and C_{DL_0}/C_{DT_0} are the leading and trailing vehicles drag coefficient in isolation respectively.

Rank	Leading Vehicle	Trailing Vehicle	$\frac{C_{DL}+C_{DT}}{C_{DL_0}+C_{DT_0}}$	Inter-Vehicle Spacing
1	EB	EB	0.780	0.25 L
2	EB	FB	0.831	0.25 L
3	EB	EB	0.852	0.50 L
4	EB	EB	0.875	0.75 L
5	EB	EB	0.885	1.00 L
6	NB	EB	0.892	0.25 L
7	FB	EB	0.893	0.25 L
8	EB	FB	0.910	0.50 L
9	EB	NB	0.930	0.50 L
10	EB	NB	0.930	0.75 L
11	EB	NB	0.931	0.25 L
12	EB	FB	0.940	0.75 L
13	EB	NB	0.945	1.00 L
14	NB	EB	0.950	0.50 L
15	EB	FB	0.951	1.00 L
16	FB	EB	0.953	0.50 L
17	NB	EB	0.956	0.75 L
18	FB	EB	0.957	0.75 L
19	FB	FB	0.957	0.25 L
20	FB	NB	0.958	0.25 L
21	NB	FB	0.960	0.25 L
22	NB	NB	0.961	0.25 L
23	NB	EB	0.963	1.00 L
24	FB	EB	0.974	1.00 L
25	FB	NB	1.013	0.50 L
26	NB	NB	1.014	0.75 L
27	NB	FB	1.017	0.75 L
28	NB	NB	1.020	0.50 L
29	NB	NB	1.020	1.00 L
30	FB	NB	1.022	0.75 L
31	NB	FB	1.024	0.50 L
32	NB	FB	1.024	1.00 L
33	FB	FB	1.025	0.50 L
34	FB	FB	1.025	0.75 L
35	FB	NB	1.028	1.00 L
36	FB	FB	1.033	1.00 L

It is important to note that for many pairs that achieve favourable energy savings (i.e., ranked < 24 in Table 3), the trailing vehicle would likely have higher drag than when being driven in isolation, leading to higher fuel consumption for that vehicle throughout a driving cycle. A solution to address this challenge without necessarily optimising the vehicle geometry either by passive or active means would be to adopt strategies from nature [29] or pelotons [30], where the platoon pair would share the leading position

equally over the total travel distance of a platoon. Adopting such a strategy would result in the drag savings calculated in Table 3 for each vehicle, which are not substantial in some scenarios, but would be expected to improve further when coupled with active aerodynamics tailored for platooning.

These observations contradict the *slip-streaming effect* as it is commonly understood, however, it agrees with remarks made by other researchers on platoons of vehicles in pairs [5,7,8,13,16,23,31]. This suggests that the *slip-streaming effect* is not universal and is highly dependent on the chosen geometry and distance between these geometries, which may help explain the misconceptions associated with this term.

Comparing the performance of the optimum pair of vehicles in platoon against much longer platoons of five to eight vehicles has been summarised in Table 4. It is observed that increasing the number of vehicles in a platoon does not guarantee a better performance of the system, as some vehicles would experience higher drag than when being driven in isolation. Even for an NB DrivAer model of seven vehicles, the improvement in drag is relatively small compared to a pair of EB geometries. Arguably having more vehicles in platoon means that more vehicles can benefit from platooning, however, pairing provides a highly effective approach to energy saving, reduction of emissions, and EV range extension without the technical and legislative complexity associated with long platoons.

Table 4. Summary of potential drag savings of different geometries in a platoon of different sizes. C_{D_i} is the drag coefficient corresponding to the vehicle location within the platoon and C_{D_0} is the drag coefficient of the vehicle in isolation.

Geometry Type	Inter-Vehicle Spacing (L)	Number of Vehicles (N)	$\frac{\sum_i^N C_{D_i}}{N \times C_{D_0}}$
DrivAer Estateback	0.25	2	0.78
DART [31]	0.17	5	0.93
Idealistic Van [11]	0.5	6	0.86
DrivAer Notchback [31]	0.22	7	0.76

4. Conclusions

This paper presents CFD results from three base geometries of the DrivAer model, the estateback, fastback, and notchback, arranged in a two-vehicle platoon in which the chosen pair, their order, and their inter-vehicle spacing were evaluated. The computational model was validated against experimental measurements.

The FB and NB geometries in isolation indicated relatively similar drag coefficients and wake structures with minor differences, particularly on the rear slanted window. A large recirculation bubble on the lower edge of the rear window was observed on the NB geometry, whilst two smaller separation bubbles were found on the upper and lower parts of the rear window on the FB geometry. In contrast, the EB geometry exhibits a much larger wake, analogous to squareback geometries where the flow immediately separates at the edge of the rear roof spoiler and extends much further downstream of the vehicle compared to the two other geometries. As such, the EB produces the highest drag coefficient followed by the FB and NB geometries, respectively.

In pairs, the vehicles leading the platoon regardless of base geometry were predicted to achieve energy savings at all the tested inter-vehicle spacing. The magnitude of these savings was much higher for the EB geometry compared to the FB and NB geometries which produced very similar figures. However, considering the pre-existing lower drag values for the FB and NB geometries, any increase in energy savings is considered more significant compared to the EB geometry. Although the EB has the highest drag, the popularity of SUVs with EB characteristics makes it highly relevant.

Vehicles in the trailing position in the majority of tested scenarios would have unfavourable results, as the drag coefficient exceeds the baseline value. The exception to this is the EB geometry in several configurations where it is following another EB geometry (at

all tested inter-vehicle spacing) or following the FB or NB at inter-vehicle spacing greater than 0.75 L.

As a coupled system, an EB geometry would be favourable as it provides the platoon with the desired drag savings irrespective of the other vehicle geometry. This drag reduction is further enhanced if the spacing between the vehicles is reduced. On the other hand, for FB and NB geometries in a platoon, the energy savings would only occur for the system when the vehicle spacing is 0.25 L or potentially lower. All other combinations of the FB and NB geometries would result in higher drag coefficients than if these vehicle shapes were operating in isolation. Several techniques can be adopted for the following vehicles such as pelotons, where the vehicle pair would lead the platoon equally throughout a driving cycle to achieve energy savings without geometrical optimisation.

If optimised, pairing provides a highly effective approach to saving energy, reduction of emissions, and EV range extension without the technical and legislative complexity associated with long platoons.

Author Contributions: Conceptualization, H.E. and R.D.; methodology, H.E.; validation, H.E.; formal analysis, H.E.; writing—original draft preparation, H.E. and R.D.; writing—review and editing, H.E. and R.D.; visualization, H.E. All authors have read and agreed to the published version of the manuscript.

Funding: This research received no external funding.

Institutional Review Board Statement: Not applicable.

Informed Consent Statement: Not applicable.

Acknowledgments: The authors would like to thank Northumbria University for granting access to the university cluster to run the simulations.

Conflicts of Interest: The authors declare no conflict of interest.

References

1. Antonelli, G.; Chiaverini, S. Kinematic Control of Platoons of Autonomous Vehicles. *IEEE Trans. Robot.* **2006**, *22*, 1285–1292. [[CrossRef](#)]
2. Dávila, A.; Nombela, M. Sartre-Safe Road Trains for the Environment Reducing Fuel Consumption through Lower Aerodynamic Drag Coefficient. SAE Technical Paper 2011-36-0060. 2011. Available online: <https://www.sae.org/publications/technical-papers/content/2011-36-0060/> (accessed on 12 October 2021).
3. Proch, A. By 2030, One in 10 Vehicles Will Be Self-Driving Globally. 2020. Available online: https://www.statista.com/press/p/autonomous_cars_2020/ (accessed on 21 September 2021).
4. Iliiafar, A. LIDAR, Lasers, and Logic: Anatomy of an Autonomous Vehicle. 2013. Available online: <https://www.digitaltrends.com/cars/lidar-lasers-and-beefed-up-computers-the-intricate-anatomy-of-an-autonomous-vehicle/> (accessed on 21 September 2021).
5. Ebrahim, H.; Dominy, R.; Martin, N. Aerodynamics of electric cars in platoon SAGE publications. *Proc. Inst. Mech. Eng. Part D J. Automot. Eng.* **2021**, *235*, 1396–1408. [[CrossRef](#)]
6. Gould, B.; Zhang, S. These 14 Companies Dominate the World's Auto Industry. 2018. Available online: <https://www.businessinsider.com/biggest-car-companies-in-the-world-details-2018-2?r=US&IR=T> (accessed on 21 September 2021).
7. Ebrahim, H.; Dominy, R. Wake and surface pressure analysis of vehicles in platoon. *J. Wind Eng. Ind. Aerodyn.* **2020**, *201*, 104144. [[CrossRef](#)]
8. Cerutti, J.; Cafiero, G.; Iuso, G. Aerodynamic drag reduction by means of platooning configurations of light commercial vehicles: A flow field analysis. *Int. J. Heat Fluid Flow* **2021**, *90*, 108823. [[CrossRef](#)]
9. Pagliarella, R. On the Aerodynamic Performance of Automotive Vehicle Platoons Featuring Pre and Post-Critical Leading Forms. Ph.D. Thesis, RMIT University, Melbourne, Australia, September 2009.
10. Le Good, G.; Resnick, M.; Boardman, P.; Clough, B. An Investigation of Aerodynamic Effects of Body Morphing for Passenger Cars in Close-Proximity. *Fluids* **2021**, *6*, 64. [[CrossRef](#)]
11. Schito, P.; Braghin, F. Numerical and Experimental Investigation on Vehicles in Platoon. *SAE Int. J. Commer. Veh.* **2012**, *5*, 63–71. [[CrossRef](#)]
12. Gan, E.C.J.; Fong, M.; Ng, Y.L. CFD Analysis of Slipstreaming and Side Drafting Techniques Concerning Aerodynamic Drag in NASCAR Racing. *CFD Lett.* **2020**, *12*, 1–16. [[CrossRef](#)]
13. Jacuzzi, E.; Granlund, K. Passive flow control for drag reduction in vehicle platoons. *J. Wind. Eng. Ind. Aerodyn.* **2019**, *189*, 104–117. [[CrossRef](#)]

14. Browand, F.; Hammache, M. *The Limits of Drag Behavior for Two Bluff Bodies in Tandem*; SAE Technical Paper; SAE 2004 World Congress & Exhibition: Detroit, MI, USA, 2004.
15. Gheysens, T.; Van Raemdonck, G. Effect of the Frontal Edge Radius in a Platoon of Bluff Bodies. *SAE Int. J. Commer. Veh.* **2016**, *9*, 371–380. [[CrossRef](#)]
16. Le Good, G.; Resnick, M.; Boardman, P.; Clough, B. *Effects on the Aerodynamic Characteristics of Vehicles in Longitudinal Proximity Due to Changes in Style*; SAE Technical Paper 2018-37-0018; CO2 Reduction for Transportation Systems Conference: Turin, Italy, 2018.
17. Heft, A.I.; Indinger, T.; Adams, N.A. *Introduction of a New Realistic Generic Car Model for Aerodynamic Investigations*; SAE Technical Paper 2012-01-0168; SAE 2012 World Congress & Exhibition: Detroit, MI, USA, 2012.
18. Varney, M.; Passmore, M.; Wittmeier, F.; Kuthada, T. Experimental Data for the Validation of Numerical Methods: DrivAer Model. *Fluids* **2020**, *5*, 236. [[CrossRef](#)]
19. Yazdani, R. Steady and Unsteady Numerical Analysis of the DrivAer Model. Master's Thesis, Department of Applied Mechanics, Chalmers University of Technology, Gothenburg, Sweden, 2015.
20. Ashton, N.; Revell, A. *Comparison of RANS and DES Methods for the DrivAer Automotive Body*; SAE Technical Paper 2015-01-1538; SAE 2015 World Congress & Exhibition: Detroit, MI, USA, 2015.
21. Wieser, D.; Schmidt, H.J.; Müller, S.; Strangfeld, C.; Nayeri, C.; Paschereit, C. Experimental Comparison of the Aerodynamic Behavior of Fastback and Notchback DrivAer Models. *SAE Int. J. Passeng. Cars Mech. Syst.* **2014**, *7*, 682–691. [[CrossRef](#)]
22. Strangfeld, C.; Wieser, D.; Schmidt, H.J.; Woszidlo, R.; Nayeri, C.; Paschereit, C. *Experimental Study of Baseline Flow Characteristics for the Realistic Car Model DrivAer*; SAE Technical Paper 2013-01-1251; SAE 2013 World Congress & Exhibition: Detroit, MI, USA, 2013.
23. Jakirlic, S.; Kutej, L.; Hanssmann, D.; Basara, B.; Tropea, C. *Eddy-resolving Simulations of the Notchback 'DrivAer' Model: Influence of Underbody Geometry and Wheels Rotation on Aerodynamic Behaviour*; SAE Technical Paper 2016-01-1602; SAE 2016 World Congress and Exhibition: Detroit, MI, USA, 2016.
24. John, M.; Buga, S.; Monti, I.; Kuthada, T. *Experimental and Numerical Study of the DrivAer Model Aerodynamics*; SAE Technical Paper 2018-01-0741; WCX World Congress Experience: Detroit, MI, USA, 2018.
25. Zabat, M.; Stabile, N.; Frascaroli, S.; Browand, F. *Drag Forces Experienced by 2, 3 and 4-Vehicle Platoons at Close Spacings*; SAE Technical Paper 950632; International Congress & Exposition: Detroit, MI, USA, 1995.
26. Davila, A.; Aramburu, E.; Freixas, A. Making the Best Out of Aerodynamics: Platoons. SAE Technical Paper 2013-01-0767. 2013. Available online: <https://www.sae.org/publications/technical-papers/content/2013-01-0767/> (accessed on 12 October 2021).
27. Tsuei, L.; Savaş, Ö. Transient aerodynamics of vehicle platoons during in-line oscillations. *J. Wind Eng. Ind. Aerodyn.* **2001**, *89*, 1085–1111. [[CrossRef](#)]
28. Watkins, S.; Vio, G. The effect of vehicle spacing on the aerodynamics of a representative car shape. *J. Wind Eng. Ind. Aerodyn.* **2008**, *96*, 1232–1239. [[CrossRef](#)]
29. Waldron, P. Why Birds Fly in a V Formation. 2014. Available online: <https://www.science.org/content/article/why-birds-fly-v-formation-rev2> (accessed on 21 September 2021).
30. Blocken, B.; van Druenen, T.; Toparlar, Y.; Malizia, F.; Mannion, P.; Andrienne, T.; Marchal, T.; Geert-Jan, M.; Jan Diepen, J. Aerodynamic drag in cycling pelotons: New insights by CFD simulation and wind tunnel testing. *J. Wind Eng. Ind. Aerodyn.* **2018**, *179*, 319–337. [[CrossRef](#)]
31. Kaluva, S.T.; Pathak, A.; Ongel, A. Aerodynamic Drag Analysis of Autonomous Electric Vehicle Platoons. *Energies* **2020**, *13*, 4028. [[CrossRef](#)]